12-2003

A Preliminary Study of the Effects of Exposure to a One Atmosphere Uniform Glow Discharge Plasma (OAUGDPTM) on the Surface Energy and Strength of Meltblown and Nanofiber Fabrics

Weiwei Chen
University of Tennessee - Knoxville

To the Graduate Council:

I am submitting herewith a thesis written by Weiwei Chen entitled "A Preliminary Study of the Effects of Exposure to a One Atmosphere Uniform Glow Discharge Plasma (OAUGDPTM) on the Surface Energy and Strength of Meltblown and Nanofiber Fabrics." I have examined the final electronic copy of this thesis for form and content and recommend that it be accepted in partial fulfillment of the requirements for the degree of Master of Science, with a major in Electrical Engineering.

J. Reece Roth, Major Professor

We have read this thesis and recommend its acceptance:

Peter P. Tsai, Marshall Pace

Accepted for the Council:
Carolyn R. Hodges

Vice Provost and Dean of the Graduate School

(Original signatures are on file with official student records.)

To the Graduate Council:

I am submitting herewith a thesis written by Weiwei Chen entitled "A Preliminary Study of the Effects of Exposure to a One Atmosphere Uniform Glow Discharge Plasma (OAUGDP^{TM}) on the Surface Energy and Strength of Meltblown and Nanofiber Fabrics". I have examined the final electronic copy of this thesis for form and content and recommend that it be accepted in partial fulfillment of the requirements for the degree of Master of Science, with a major in Electrical Engineering.

J. Reece Roth
Major Professor

We have read this thesis
and recommend its acceptance:

Peter P. Tsai

Marshall Pace

Accepted for the Council:

Anne Mayhew
Vice Provost and
Dean of Graduate Studies

Original signatures are on file with official student records.

A Preliminary Study of the Effects of Exposure to a One Atmosphere Uniform Glow Discharge Plasma (OAUGDP^{TM}) on the Surface Energy and Strength of Meltblown and Nanofiber Fabrics

A Thesis
Presented for the
Master of Science
Degree
The University of Tennessee, Knoxville

Weiwei Chen
December 2003

ACKNOWLEDGEMENT

This work was supported in part by the National Science Foundation (NSF) Nanoscale Exploratory Research (NER) grant, NSF-NER DMI-0210554, titled "*NER: Increasing the Strength, Surface Energy, and Wickability of Polymeric Nanofabrics by Exposure to a One Atmosphere Uniform Glow Discharge Plasma (OAUGDP)*", and in part by the University of Tennessee Center for Materials Processing, Dr. Carl McHargue, Director.

I would like to express my heartfelt gratitude to my advisor, Professor J. Reece Roth for his guidance throughout the Master's program. His insights, and advice not only increase my academic success, but more importantly help me develop as a better person in the future. I am also very grateful for Dr. Peter P. Tsai's knowledgeable instructions during this research. Great thanks are also owed to Professor Marshall O. Pace for his valuable advice in my research and thesis reviewing.

Further thanks are extended to Professor Michael L. Keene, the class of English 462 "Writing for Publication", staff at the UT Textiles and Non-woven Development Center and the Department of Material Science & Engineering Research Facilities.

ABSTRACT

Electrohydrodynamic (EHD) methods have recently been developed to electrospin nano-scale non-woven webs and to improve their properties by exposure to the One Atmosphere Uniform Glow Discharge Plasma (OAUGDP™), as a collaborative effort by the UT Plasma Sciences Laboratory and the UT Textiles and Nonwovens Development Center (TANDEC).

Nanofiber webs are made by the *electrospinning* (ES) process, which uses the electrostatic force to spin fibers from a polymer solution or melt. Digitized SEM images show that the fiber diameters range from 10 nm to several microns. Such nanofiber fabrics have a significantly higher tensile strength than meltblown (MB) webs of the same material composed of fibers microns in diameter. Nanofiber fabrics also require less energy input and may require less capital investment when compared to the traditional meltblown process. These webs can be post-treated by exposure to the One Atmospheric Uniform Glow Discharge Plasma (OAUGDP^{TM}) to improve surface characteristics such as wettability and wickability. This paper reports for the first time that a durable high surface energy has been achieved on Nylon meltblown microfiber fabrics by exposure to OAUGDP^{TM}.

This paper discusses possible chemical and physical mechanisms responsible for these property changes, based on analysis of scanning electron microscopy (SEM) images. Some recent efforts in both nanofiber generation and plasma reactor technology are discussed as well. With future development, these improved nanofiber fabrics should find applications to protective garments and other clothing.

* This research is supported by NSF grant DMI-0210554 of the Nanoscale Science and Engineering Initiative, NSF 01-157, Dr. Janet M. Twomey, program manager.

TABLE OF CONTENT

LIST OF TABLES

LIST OF FIGURES

CHAPTER I. INTRODUCTION

Fibers used in fabrics for garments and other domestic purposes can be classified as either natural or artificial in their origin. The natural fibers are further divided into those of animal origin, which contain protein, e.g., wool, fur, etc., and those of plant origin, which are cellulose-based, like cotton, linen, and others. Figure 1 shows a natural fiber producer.

Fabrics can be categorized by the method of assembling the fibers into a fabric, into either wovens or non-wovens. Woven textiles are formed by interlacing fibers with each other in a systematic order. Non-wovens, however, are an assembly of fibers held together by mechanical interlocking in a random web or mat, by fusing the fibers, or by bonding with a cementing medium.

Currently there are two commercially dominant non-woven manufacturing methods. One is spunbond, which directly converts polymer into continuous filaments, and the filaments into a randomly laid fabric by thermal bonding. Meltblowing (MB) is a second process in which a fibrous web is produced directly from polymers or resins using high-velocity air to attenuate the filaments and attach them to each other. Historically, meltblowing technology was first developed under U.S. government sponsorship in the Naval Research Laboratory in the early 1950s [Haynes 1991], but it wasn't until the 1970s that the technology was commercialized.

Figure 1 Protein-based Natural Producer

Table 1 Diameter of Selected Natural and Artificial Fibers

Material	Diameter Mean Value (microns)	Coeff. Variantion (%)
Spider silk	3.57	14.8
B. mori Silk	12.90	24.8
Merino Wool	25.50	25.6
Polyester	13.30	2.4
Nylon 6 Filament	16.20	3.1
Kevlar 29	13.80	6.1

Table 1 lists the diameter of some selected natural and artificial fibers as well as the coefficients of variation [Ko et al. 2002]. These diameters are smaller than that of a human hair, which characteristically ranges from 50 to 150 microns, but even spider silk is in the micron range.

To further understand the structural differences between these fabrics, including electrospun fabrics, scanning electron microscopy (SEM) images of silk, denim (a hard-wearing woven cotton cloth), spunbond, and meltblown fabrics are given in Figure 2 [Noll 2000, Zhang et al. 2002]. SEM is an important diagnostic method to visualize the surface topography of fabrics for scientific assessment of physical effects on fabric surfaces. More about SEM will be discussed in later chapters.

It is important to notice that those natural fabrics are produced at room temperature, from natural feedstocks, with a relatively low energy input, and without capital equipment, while the artificial fibers listed are produced under generally opposite conditions. For instance, the 1-meter Reicofil 2 Spunbond Line at the UT Textiles and Non-wovens Development Center, shown in Figure 3 (http://tandec.utk.edu), works at temperatures varying from 240 to 280 ˚C**,** and requires 2 persons to maintain production. This equipment cost six million U.S. dollars initially. Therefore, there should be great improvement in energy conservation and capital investment savings, if science and engineering can successfully learn from nature and generate fibers and fabrics in a manner that is industrially feasible.

The rapid production of large quantities of nanoscale fibers is possible through electrospinning (ES) technology. Fibers with diameters ranging from 10 to 1000 nanometers have recently been produced efficiently at room temperature, and with minimal energy input. The same process can also

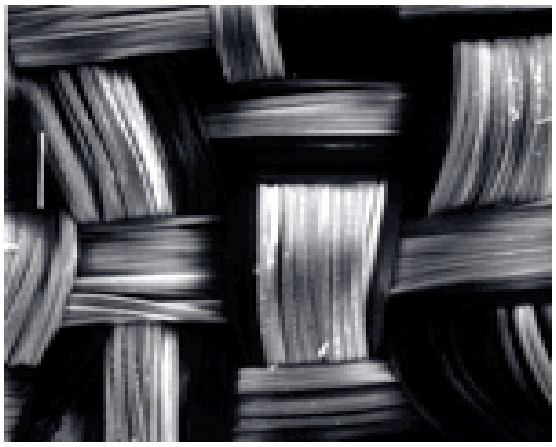

(a) Silk

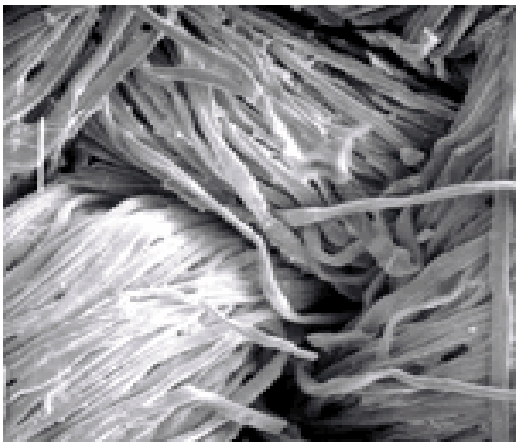

(b) Denim

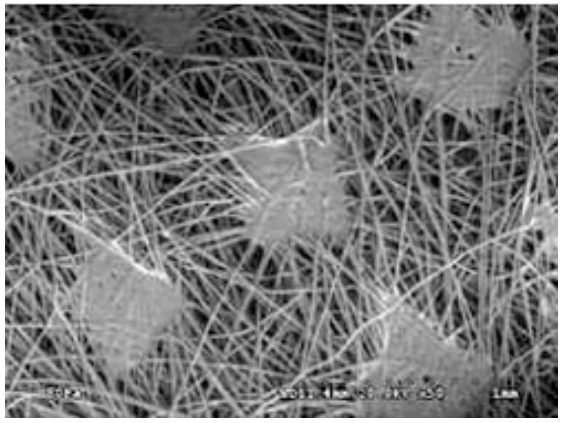

(c) Spunbond

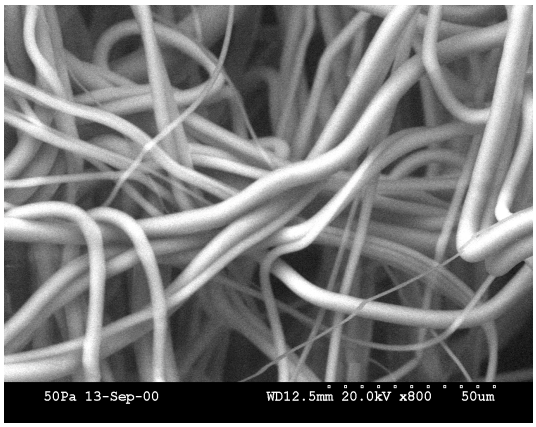

(d) Meltblown

Figure 2 SEM Images of Fabrics: (a) Silk (b) Denim (c) Spunbond and (d) Meltblown

Figure 3 1-meter Reicofil 2 Spunbonding Line at TANDEC

form fabrics without additional equipment. Such nanofiber fabrics possess many interesting features.

In order to provide a frame of reference for our results on nanofiber fabrics, we have also taken data on conventional meltblown (MB) fabrics. To distinguish the meltblown from the electrospun nanofiber fabrics, the former are called “microfiber fabrics” because their fiber diameters are on the order of microns.

CHAPTER II. PRINCIPLE OF ELECTROSPINNING TECHNOLOGY FOR POLYMERIC NANOFIBER FABRICS

Electrospinning (ES) is a process that uses the electrostatic force to charge a polymer solution or melt, and spin fibers from these polymer clusters, as shown in Figure 4. The nozzle (*spinneret*) is at high voltage, and the collector plate is normally at ground potential. As the solution droplet is formed at the spinneret, driven by a low flow pump, the applied electric field is sufficiently high so as to overcome the surface tension force of the droplet and generate polymer jets. As a free charged jet leaves its original surface, it will be dragged along with the charge toward a grounded collector. The electric forces continue to stretch the polymer jet as it flows away, and the jet will split multiple times into a plurality of thinner fibers (the *splay*) until it reaches the target, where an interconnected web of fine filaments is eventually formed. An interesting and important feature of this process is that, like spiders in nature, the fibers are produced at room temperature rather than at temperatures high enough to keep the polymers in a molten state, as in the processes of meltblowing or spun-bonding.

This method of producing man-made fibers has been known since 1934, when the first patent was filed by A. Formhals (1934). He suggested the use of one electrode as an efficient collector for electrospun fibers. Over 30 patents and many publications have been reported since then. The significant characteristics of electrospun (ES) fibers are their small diameter and uniform fiber size. Electrospun fibers in the size range of 0.1 to 0.7 microns from

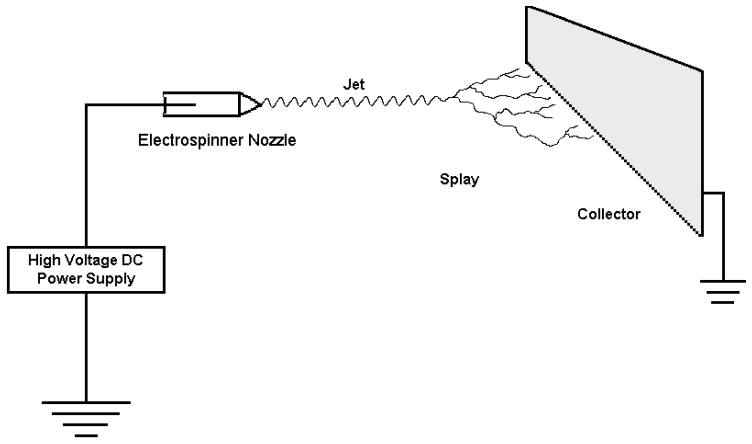

Figure 4 Schematic Representation of the Electrospinning Process

polymers including polycarbonate, poly (ethylene oxide), polyurethane, polystyrene, polycaprolactone, and polystyrene (just to name a few here) have been studied [Tsai et al. 2001b, 2002a]. The fiber diameter and the web formation mechanisms are determined by several parameters, such as the polymer and solvent types, the polymer solution concentration, the applied electrical voltage to the spinneret, the distance between the spinneret and the fiber collector, and the spinning throughput rate. More importantly, Tsai, et al (2001a) reported that the fiber spinning rate, the web formation mechanisms, and the web properties such as density, uniformity and strength were greatly improved by controlling the external electric field strength between the spinneret and the collector.

When the diameters of electrospun polymeric fibers are less than 500 nanometers, nanofiber fabrics have a very soft hand; their polymeric materials are recyclable; and such fabrics may be permeable to air and water vapor, but not to microorganisms or fine particles because of their small distance between adjacent fibers. These qualities make them very promising for both fashionable and utilitarian garments, especially protective clothing. However, current commercial applications of nanofiber fabrics are only found in ultra high efficiency filtration webs. Freudenberg Nonwovens in Germany has been electrospinning for over 20 years, producing electrospun filter media from a continuous web feed for high-end filter markets. Small companies are now beginning to develop this technology in the United States, including eSpin Technologies in Chattanooga, Tennessee and Foster Miller Inc in Waltham, Massachusetts [Schreuder-Gibson et al. 2000]. The challenges facing further development of electrospinning technology are discussed below.

The strength of electrospun nanofiber webs has been comparable to that of a meltblown web, whose strength is medium-to-low compared with other non-woven fabrics. For applications such as filter media, such strength is adequate because the filter media can be easily supported by laminating with other fabrics having higher strength. However, some applications such as protective garments require higher strength. Because the ES filter media has the advantage of a large surface area associated with their fine fibers [Schmidt 1980, Weghmann 1982, Davis 1987], the possibility of using the ES polyurethane for military protective clothing due to its excellent elasticity has been investigated [Shreuder-Gibson et al. 2000]. However, its strength is about half (9.6 MPa) that of the cast film (15.8 Mpa) made of the same material. The authors of the same paper [Shreuder-Gibson et al. 2000]

commented that it is important to obtain greater strength of ES materials through further modification by post-treatment.

In addition to the web strength, the moisture vapor transmission rate, or the water vapor diffusion resistance, is a second important parameter for protective garments because it determines the body heat dissipation rate by water vapor ventilation. The moisture vapor transmission rate is governed by the web pore size and the hydrophilicity of the web; the larger the pore size and the higher the hydrophilicity of the material, the higher the vapor ventilation ability. However, the pore size of protective garment material is minimized in order to improve such protective properties as reduction in the penetration of wind, bacteria, and chemical vapors. Gibson et al. (1999) showed that for hydrophilic materials, the water vapor diffusion resistance was reduced at high relative humidity conditions due to higher web moisture content. Hydrophilicity is a polymeric property. However, the hydrophilicity of a polymer can be greatly increased and made durable by plasma treatment, as will be discussed later.

Potential applications of nanofiber fabrics include filter media, protective garments, a hydrogen reservoir for hydrogen fuel cells, composite reinforcement, a catalyst medium, biomaterials such as implants, bioreactors, wound dressings, drug-release capsules, etc.

There are some potential problems as well. For example, fabricating large quantities of nanofiber fabrics at commercial speeds. The dyeability of fabrics is arguable, because their fiber diameter is less than the wavelength of light and these fibers are seen by diffraction or Rayleigh scattering.

CHAPTER III. LABORATORY APPARATUS FOR ELECTROSPUN NANOFABRICS PRODUCTION

Electrospun nanofiber fabrics are produced by electrostatically elongating a polymeric fiber until it breaks up into multiple smaller fibers having diameters as small as ten nanometers.

In the National Science Foundation (NSF) Nanoscale Exploratory Research (NER) grant titled "*NER: Increasing the Strength, Surface Energy, and Wickability of Polymeric Nanofabrics by Exposure to a One Atmosphere Uniform Glow Discharge Plasma (OAUGDP)*", which supported this paper, we developed several generations of electrospinning apparatus.

Figure 5 shows the original electrospinning device in our laboratory. The electrospinning nozzle is the metallic needle of a hypodermic syringe. The high voltage wire is clipped directly to the needle, and a massive stack of bulk nanofiber material has built up in this instance. This bulk material was not used in any of the tests reported here. In later versions of the apparatus, we produced flat-sheet fabrics, shown being formed by a single jet in Figure 6 on a substrate of wax paper, which we found to be the most effective collecting method for fabric tests. The electrospinning nozzle is in the foreground.

Figure 7 shows our latest apparatus, which is moving in the direction of an industrial production prototype. The spinneret is an assembly of three hypodermic syringes, designed to produce larger area nanofiber fabrics than

Figure 5 The Electrospinning Process in Action

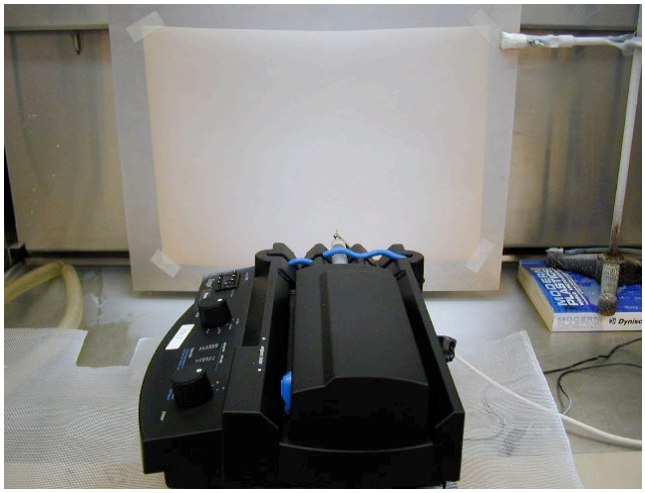

Figure 6 A Nylon Electrospinning System Equipped with a Single Hypodermic-syringe Pump and Negative Flat Plate Collector

Figure 7 Production of a Nanofiber Fabric on a Rotating Collector Drum with Three Spinnerets

are possible with a single nozzle. A common motorized plunger drives the syringes. The fibers are collected on a rotating drum so that the effect of non-uniform distribution of fibers arriving at the fabric has been averaged out.

With this system, the optimal conditions to make Nylon fibers continuously were 0.00228 ml/min throughput, an applied voltage on the syringe nozzle of +26kV, a bias voltage on the metal collector of –10kV, and a distance from the nozzle to the collector of 25 cm. For the electrospinning of polyurethane fibers, the throughput was 0.0456 ml/min, the applied voltage on the syringe nozzle was +18 kV, the bias voltage on the metal collector was –12 kV, and the distance from the nozzle to the collector was 20cm.

The majority of our work was done on two polymers, Nylon and polyurethane (PU). Nylon can be dissolved in formic acid for electrospinning and its fabric is a suitable material for garments. Polyurethane can be dissolved in dimethyl formamide (DMF) and tetrahydrofuran (THF) for electrospinning, and its fabric possesses stretchability, a useful characteristic for garments. A polymer solution of Nylon 6 was prepared by dissolving 15% Nylon solid by weight in formic acid. Polyurethane solution was prepared by dissolving 20% PU solid by weight at 1:1 ratio of THF:DMF. Other materials we made into nanofiber fabrics are polyacrylonitrile (PAN), polycaprolactone (PCL), and polycarbonate (PC). The SEM analyses of the fabrics made of these polymers are in the next chapter.

CHAPTER IV. SEM ANALYSES OF FIBER DIAMETER DATA

Scanning electron microscopy (SEM) is one of the most widely used diagnostic methods in modern materials science and processing. In this method, electrons instead of photons are used as a probe to scan the surface topography and produce an image in a way similar to that of a television. Its best resolution can be in the range of an atomic diameter, tenths of a nanometer, which means that workpieces can be examined at a very high magnification. The SEM also allows a greater depth of focus than an optical microscope so that it provides a good representation of three-dimensional samples.

Figure 2 has already shown the SEM images of silk, denim, PTT spunbond, and PP meltblown fabrics. The textures of fibers are closely related to the macroscopic strength of the fabrics [Noll, 2000]. For example, silk and denim have very high strength and correspondingly their fiber structures are very highly ordered.

In our research, a Leo 1525 workstation manufactured by the Carl Zeiss SMT AG Company (http://www.leo-em.co.uk/) is used to produce digital images of fabrics after their production by meltblowing or electrospinning. It has an ultra high resolution (1.5 nm at 20 kV acceleration voltage and 3.5 nm at 1 kV) and the possibility to vary electron beam energies, which is especially important for non-conducting materials.

Figure 8 shows SEM images of meltblown and electrospun Nylon fabrics, respectively. Figure 9 contains images of meltblown and electrospun polyurethane (PU) fabrics. The meltblown fabrics in both figures look like a plate of spaghetti; most of the fibers are loosely attached to each other and some groups of fibers are just bundled together in a few parallel strands. There is little twisting and no knotting observed. However, the electrospun fabrics more resemble a network with many nodes. The fibers appear to be knotted, twisted, or otherwise joined at the nodes of the network. Beyond this, the individual electrospun nanofibers appear to be randomly woven under-and-over each other. Both the attachment at nodes and the woven texture of the nanofiber fabrics could strengthen them compared to the meltblown fabrics of Figures 6a and 7a, which lack these features.

Figure 10 gives the SEM images of electrospun fabrics of polyacrylonitrile (PAN), polycaprolactone (PCL), and polycarbonate (PC), respectively. They show similar patterns of twisting, interweaving, and

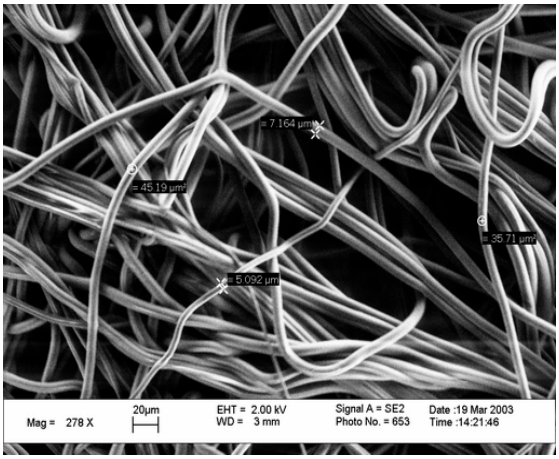

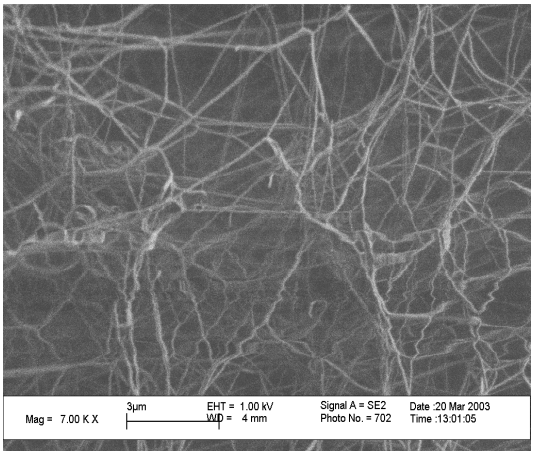

(a) Nylon microfibers **(b) Nylon nanofibers**

Figure 8 Scanning Electron Micrographs (SEM) of Two Nylon Fabrics: (a) Meltblown Nylon 6 – note 20 micron fiduciary marker at lower left (b) Electrospun Nylon 6-6 – note 3 micron fiduciary marker at lower left.

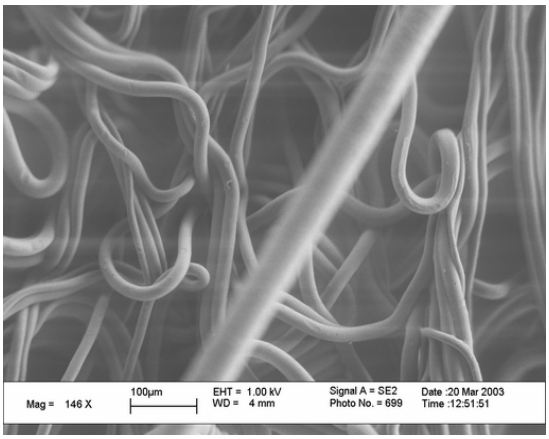

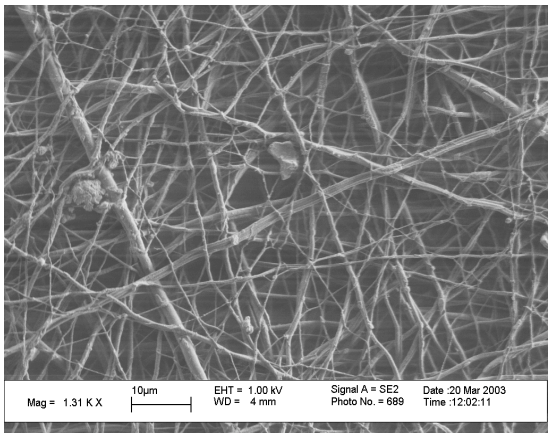

(a) PU microfibers **(b) PU nanofibers**

Figure 9 SEM of Two Polyurethane (PU) Fabrics: (a) meltblown polyurethane (PU) with human hair diagonally in the foreground (b) Electrospun polyurethane (PU).

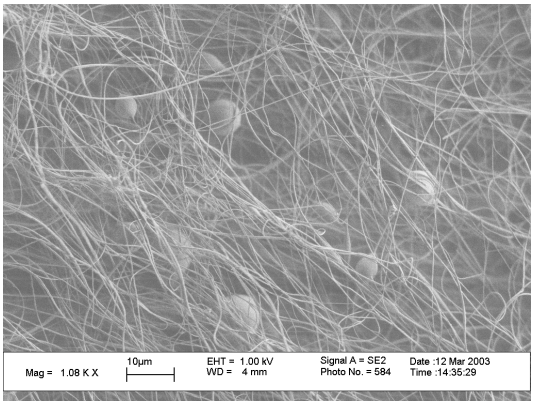

(a) PAN

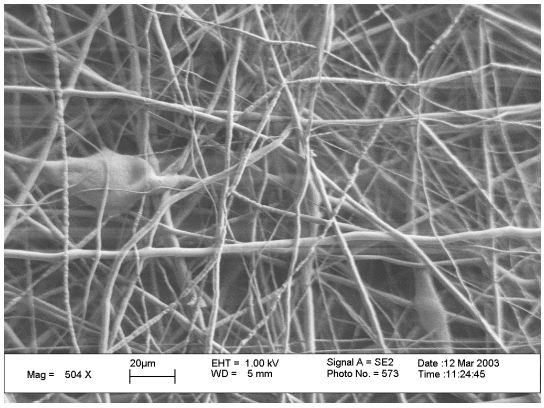

(b) PCL

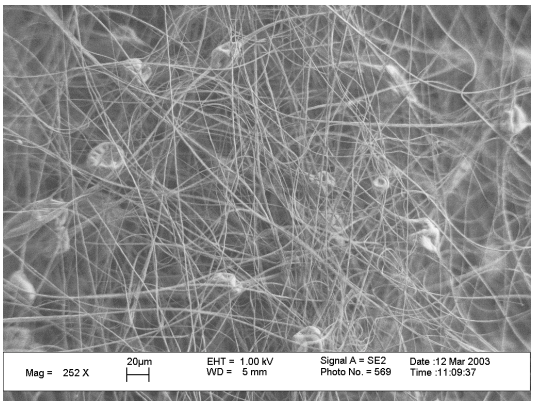

(c) PC-2

Figure 10 SEM of Electrospun Fabrics: (a) PAN, (b) PCL, and (c) PC-2

knotting among the fibers. Further interesting features are found from the statistical investigation in the rest of the chapter.

The fiber diameter can be directly measured on the digital SEM images using software called Scion Image by the Scion Corporation (http://www.scioncorp.com). This software permits the investigator to identify two points at opposite ends of a fiber diameter, compare the distance to a scale provided as a standard with the SEM image, and then report the diameter. For instance, a few such designated diameters are shown in Figure 6a. These data were input into a statistical package named JMP 4 (http://www.jmp.com). Based on the fiber diameters measured, a few statistics such as mean, maximum, quantiles, etc., are calculated, the cumulative probability distributions for each sample were plotted, and histograms of the number of fibers within selected bands of fiber diameters were prepared. These plots are shown in Figures 11 to 14.

The statistical characteristics of meltblown and electrospun polyurethane fabrics are shown in Figure 11. The cumulative distribution function of the 23 meltblown fiber diameter data in 11a is consistent with a Gaussian distribution with a mean value of 19 microns and a standard deviation of 5.4 microns. The cumulative distribution function of the 40 electrospun PU fiber diameter data in Figure 11b has been fit by a Gaussian distribution with a mean value of 660 nm and a standard deviation of 370 nm. The histogram of the actual distribution function and the departures from a straight line on the probability plot of the electrospun data show significant skewness (the 3rd moment of the probability distribution function for diameter), which indicates either erroneous outliers in the observation process or an asymmetric distribution. The data may follow a Gaussian or Laplacian distribution function. More data are required in future work.

The diameter statistics of meltblown and electrospun Nylon 6 fabrics are shown in Figure 12. The cumulative distribution function of the 40 meltblown fiber diameter data in Figure 12a is consistent with a Gaussian distribution with a mean value of 6.8 microns and a standard deviation of 1.6 microns. The 13 electrospun Nylon 6 fiber diameter data in Figure 12b have a mean value of 68 nm and a standard deviation of 21 nm. Lack of sufficient data in this case makes any conclusion about the nature of the distribution function vulnerable. This occurs because when the SEM is under very high magnification, charging problems become serious on the nonconductive surfaces resulting in image drift that makes the image too “fuzzy” to make measurements. More experience in SEM operation or necessary adjustments

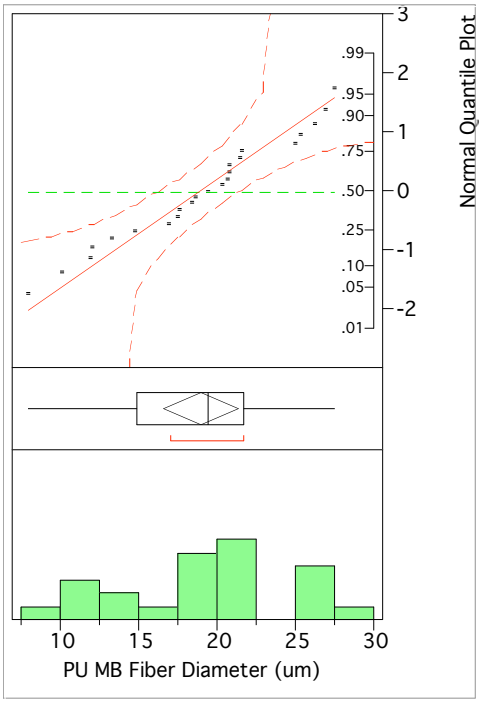

Quantiles		
100.0%	maximum	28
99.5%		28
97.5%		28
90.0%		27
75.0%	quartile	22
50.0%	**median**	**20**
25.0%	quartile	15
10.0%		11
2.5%		8.0
0.5%		8.0
0.0%	minimum	8.0

Moments	
Mean	19.0
Std Dev	5.4
Std Err Mean	1.1
upper 95% Mean	21
lower 95% Mean	17
Sample Number	**23**

(a)

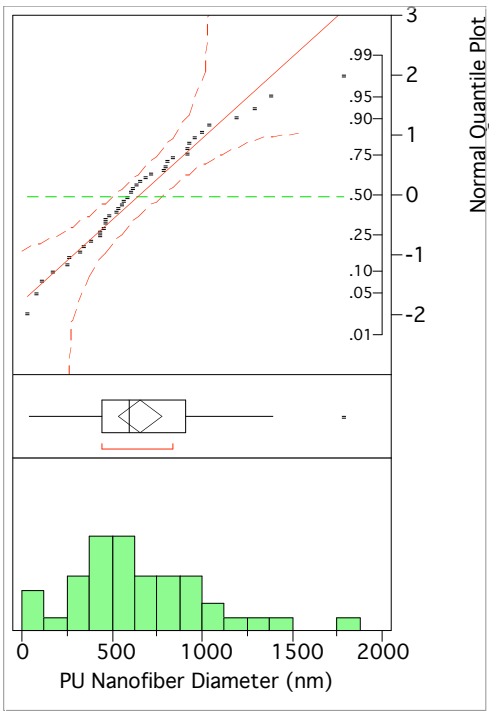

Quantiles		
100.0%	maximum	1800
99.5%		1800
97.5%		1800
90.0%		1200
75.0%	quartile	900
50.0%	**median**	**600**
25.0%	quartile	440
10.0%		180
2.5%		41
0.5%		40
0.0%	minimum	40

Moments	
Mean	660
Std Dev	370
Std Err Mean	58
upper 95% Mean	770
lower 95% Mean	540
Sample Number	**40**

(b)

Figure 11 Diameter Statistics of Meltblown and Electrospun Polyurethane (PU) Fabrics: (a) MB PU (in μm) (b) ES PU (in nm)

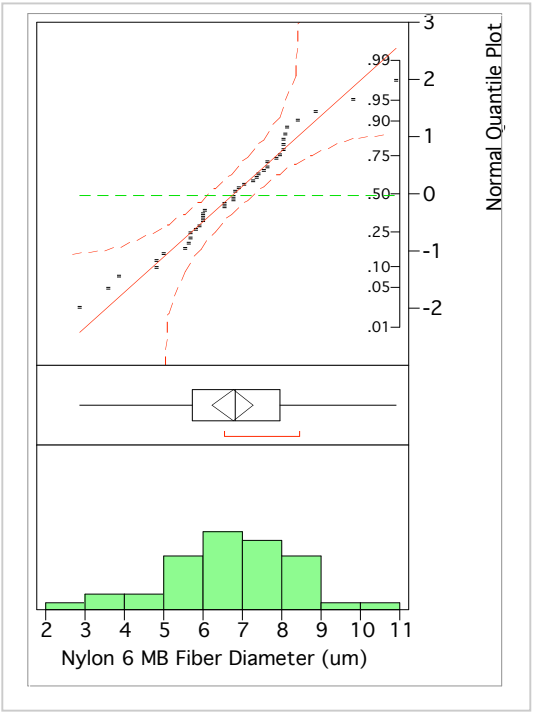

Quantiles		
100.0%	maximum	11
99.5%		11
97.5%		11
90.0%		8.4
75.0%	quartile	8.0
50.0%	**median**	**6.8**
25.0%	quartile	5.7
10.0%		4.8
2.5%		2.9
0.5%		2.9
0.0%	minimum	2.9

Moments	
Mean	6.8
Std Dev	1.6
Std Err Mean	0.26
upper 95% Mean	7.3
lower 95% Mean	6.2
Sample Number	**40**

(a)

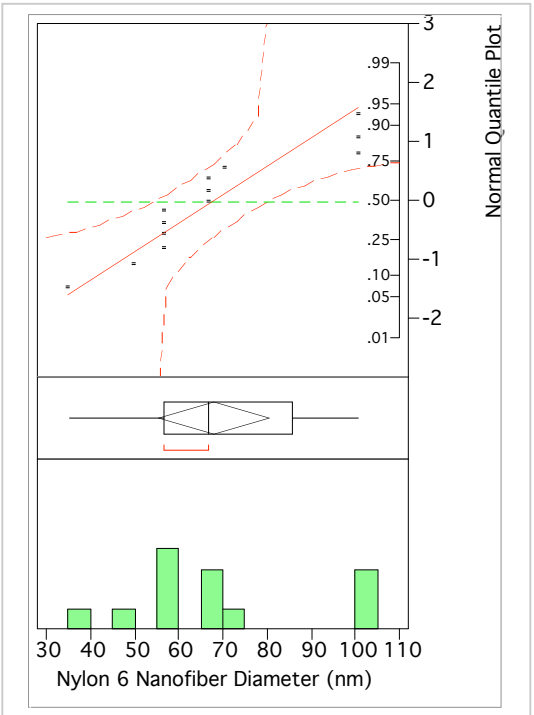

Quantiles		
100.0%	maximum	100
99.5%		100
97.5%		100
90.0%		100
75.0%	quartile	86
50.0%	**median**	**67**
25.0%	quartile	57
10.0%		41
2.5%		35
0.5%		35
0.0%	minimum	35

Moments	
Mean	68
Std Dev	21
Std Err Mean	5.8
upper 95% Mean	81
lower 95% Mean	56
Sample Number	**13**

(b)

Figure 12 Diameter Statistics of Meltblown and Electrospun Nylon Fabrics: (a) Nylon 6 MB (in um) (b) Nylon 6 ES (in nm)

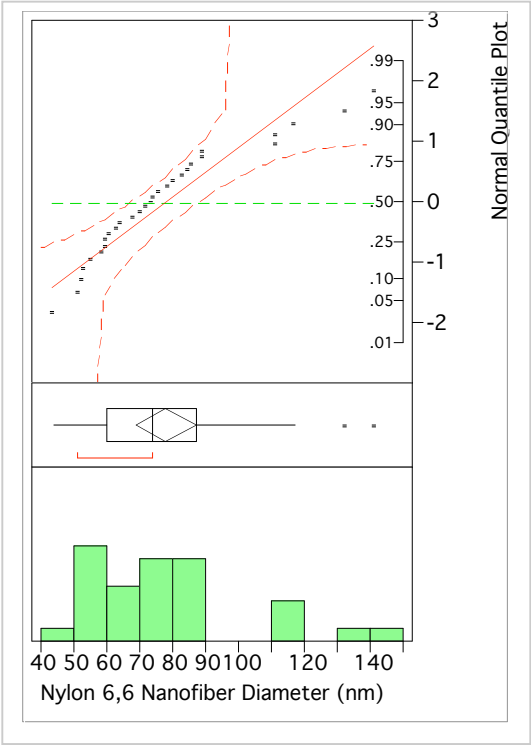

Quantiles		
100.0%	maximum	140
99.5%		140
97.5%		140
90.0%		120
75.0%	quartile	88
50.0%	**median**	**74**
25.0%	quartile	60
10.0%		53
2.5%		44
0.5%		44
0.0%	minimum	44

Moments	
Mean	78
Std Dev	25
Std Err Mean	4.6
upper 95% Mean	87
lower 95% Mean	69
Sample Number	**29**

(a)

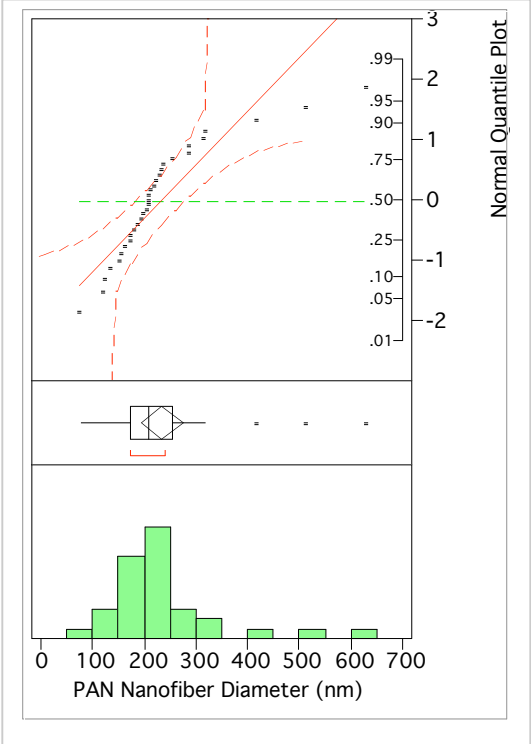

Quantiles		
100.0%	maximum	630
99.5%		630
97.5%		630
90.0%		400
75.0%	quartile	260
50.0%	**median**	**210**
25.0%	quartile	170
10.0%		130
2.5%		76
0.5%		76
0.0%	minimum	76

Moments	
Mean	240
Std Dev	110
Std Err Mean	20
upper 95% Mean	280
lower 95% Mean	190
Sample Number	**31**

(b)

Figure 13 Diameter Statistics of Electrospun (ES) Polymeric Fabrics: (a) Nylon 6-6 (in nm) (b) PAN (in nm)

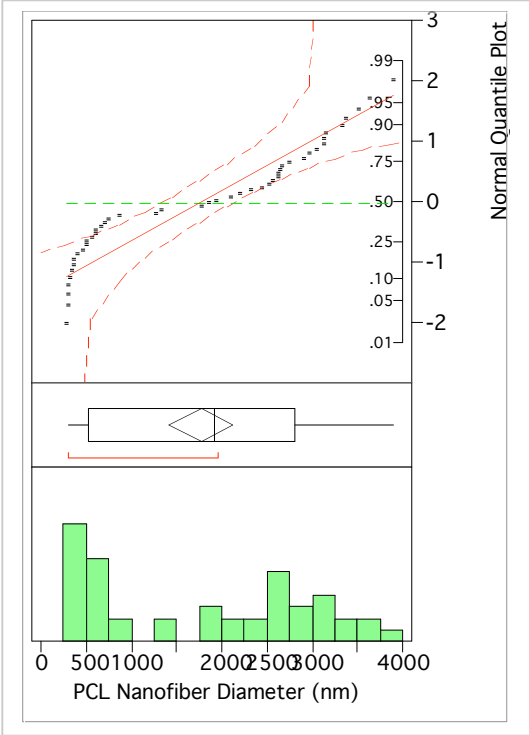

Quantiles		
100.0%	maximum	3900
99.5%		3900
97.5%		3900
90.0%		3400
75.0%	quartile	2800
50.0%	**median**	**1900**
25.0%	quartile	520
10.0%		320
2.5%		300
0.5%		300
0.0%	minimum	300

Moments	
Mean	1800
Std Dev	1200
Std Err Mean	180
upper 95% Mean	2100
lower 95% Mean	1400
Sample Number	**46**

(a)

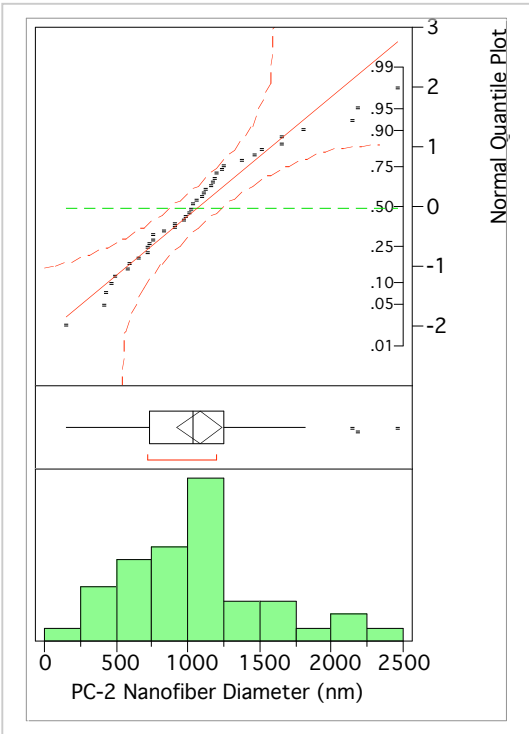

Quantiles		
100.0%	maximum	2500
99.5%		2500
97.5%		2500
90.0%		1800
75.0%	quartile	1300
50.0%	**median**	**1000**
25.0%	quartile	730
10.0%		470
2.5%		160
0.5%		160
0.0%	minimum	160

Moments	
Mean	1100
Std Dev	500
Std Err Mean	80
upper 95% Mean	1200
lower 95% Mean	920
Sample Number	**40**

(b)

Figure 14 Diameter Statistics of Electrospun (ES) Polymeric Fabrics: (a) PCL (in nm) (b) PC-2 (in nm)

to the SEM itself may solve this problem.

The diameter statistics of electrospun Nylon 6-6, polyacrylonitrile (PAN), polycaprolactone (PCL), and polycarbonate (PC-2) nanofiber fabrics are shown in Figures 13a through 14b, respectively. The cumulative distribution function of the 29 Nylon 6-6 electrospun fiber diameter data in Figure 13a has been fit by a Gaussian distribution with a mean value of 78 nm and a standard deviation of 25 nm. There is some skewness in the histogram of the electrospun data.

The cumulative distribution function of the 31 electrospun PAN fiber diameter data in Figure 13b has been fit by a Gaussian distribution with a mean value of 240 nm and a standard deviation of 110 nm. The histogram of the actual distribution function and the departures from a straight line on the probability plot of the electrospun data also suggest a non-Gaussian distribution with significant skewness.

The cumulative distribution function of the 46 electrospun PCL fiber diameter data in Figure 14a has been fit by a Gaussian distribution with a mean value of 1800 nm and a standard deviation of 1200 nm. The shape of the histogram and the departures from a straight line on the probability plot of the data indicate a non-Gaussian, and even bimodal distribution. The fiber diameters of PCL concentrate in two ranges: sub-micron and from 2 to 4 microns. Correspondingly, on the SEM image the fabric looks like a mixture of nano- and micro-scale fibers.

The diameter statistics of electrospun polycarbonate (PC-2) nanofiber fabric is shown in Figure 14b. The cumulative distribution function of the 40 electrospun PC-2 fiber diameter data in Figure 14b has been fit by a Gaussian distribution with a mean value of 1100 nm and a standard deviation of 500 nm. The histogram of the actual distribution function has a peak around 1000 nm and a considerable portion of fibers lie in the range of 500 to 1000 nm.

As a result, the statistical characteristics of the meltblown and electrospun fabrics documented in Figures 11 to 14 are summarized in Table 2, with the meltblown fabrics in the top two rows, and the electrospun fabrics below. It is evident from Table 2 that the mean diameters of electrospun fibers in Nylon and PU fabrics are from 20 to 100 times smaller than those of the meltblown fabrics. It is important to realize that the fiber diameters in Table 2 represent values that were most consistently produced, and that the largest or smallest mean diameters that the electrospinning

Table 2 Diameter Distribution Function Statistics of Micro- and Nanofiber Fabrics

Fabric Type	# points	Median	Mean	S.D.	C.V. (%)
Nylon 6 MB	40	6.8 μm	6.8 μm	1.6 μm	24 %
PU MB	23	20 μm	19 μm	5.4 μm	28 %
PU Nano	40	600 nm	660 nm	370 nm	62%
Nylon-6 Nano	13	67 nm	68 nm	21 nm	31 %
Nylon-66 Nano	29	74 nm	78 nm	25 nm	33 %
PAN Nano	31	210 nm	240 nm	110 nm	54 %
PCL Nano	46	1.9 μm	1.8 μm	1.2 μm	63 %
PC-2 Nano	40	1.0 μm	1.1 μm	0.50 μm	49 %

process is capable of are not listed, but can be found in details from Figures 11 to 14.

CHAPTER V. THE ONE ATMOSPHERE UNIFORM GLOW DISCHARGE PLASMA (OAUGDP)

Plasma is the fourth state of matter in nature, in addition to the well-known solid, liquid, and gaseous states. Plasma is defined as an approximately electrically neutral collection of ions and electrons, which may or may not contain a neutral background gas. There are many significant characteristics of plasma, which lead to broad areas of industrial application. One difference between plasma and ordinary neutral gas is that plasma responds strongly to imposed electric and magnetic fields, so that they can be manipulated, and very high energy densities can be attained. Plasmas also generate several kinds of active species, which can be more energetic than those produced in chemical reactors. These energetic active species make plasma-assisted material processing a very competitive method of modifying the properties of materials.

The area of plasma surface treatment is well established. It uses plasma exposure to change the surface energy, wettability, and bonding of fabrics, films, and solids, and it can sterilize and clean surfaces. Plasmas with too low or high number density, like the dark discharge or the plasma torch, are not generally useful for plasma processing because either not enough active species are provided, or too high an energy input will damage the material. Only glow discharge plasmas possess the appropriate density and flux of active species to be industrially useful.Conventionally, many industrial applications of glow discharge plasmas are operated at pressures below 10 torr, where a glow discharge can be stably generated and easily maintained. However, this low pressure requires expensive vacuum systems and batch processing, which increase the capital investment of processing lines, while limiting the production rate.

Over the past few years, interest has grown in applying well-known "classical" atmospheric pressure plasmas to plasma processing. These include corona discharges, dielectric barrier discharges, arcjets, and inductive plasma torches. More recent developments include the Atmospheric Pressure Plasma Jet and the One Atmosphere Uniform Glow Discharge Plasma (OAUGDP) [Roth et al. 1995a, 1995c].

Compared to other forms of atmospheric pressure plasma, the uniformity and low-to-moderate areal power densities of the glow discharge are important for surface treatment, in order to achieve a uniform effect to meet industrial requirements. The discovery of the OAUGDP is based on

the ion-trapping mechanism [Roth 2001, section 15.4]. Later results, including experimental observation and computer modeling [Ben Gadri 1999] demonstrates that the OAUGDP™ can be operated, under proper conditions, at 1 atm of pressure, and be made uniform, and free of filaments.

The early history of the OAUGDP™, which goes back to 1933, has been discussed elsewhere [von Engle et al. 1933]. At the UT Plasma Sciences Laboratory, a program to produce an atmospheric glow discharge in air was initiated in 1988, and produced a 1.6-liter OAUGDP™ between parallel plates in helium gas in January 1992, and in air a few months later. Subsequent developments allowed the OAUGDP™ to be generated in a variety of geometries, including a plane-parallel slab geometry, and a surface layer of plasma on flat panels [Roth 2001, section 17.1.3.3]. Investigation of the physical processes in the OAUGDP™ at UT identified the ion-trapping mechanism and the limitation of the operating frequency to a relatively narrow range of audio RF driving frequencies as a requirement for a stable, uniform plasma.

Characteristic areal power densities of the OAUGDP™ are a few tens of milliwatts to a few watts per square centimeter, not high enough to damage or degrade most exposed materials. Also very important to industrial applications is the fact that glow discharges are very energy efficient in maintaining themselves in an ionized state. Unobstructed normal glow discharges operate at the Stoletow point [Roth 1995b, section 17.1.3.3], at which only 81 electron volts is required to produce an ion-electron pair in air. By contrast, arcjets and plasma torches typically require an energy input of more than 10,000 eV per ion-electron pair, nearly all of which goes into heating the neutral gas instead of producing ionization or active species useful for plasma processing.

CHAPTER VI. OPERATION OF THE MOD VI OAUGDP™ REACTOR

The MOD VI OAUGDP™ parallel plate re-circulating plasma reactor was designed and developed at the UT Plasma Sciences Laboratory to perform atmospheric pressure plasma research, diagnostics, and plasma-related material processing with air at one atmosphere. A picture of the main chamber is shown in Figure 15, with the plasma energized.

The atmospheric plasma is generated in a stainless steel chamber with interior dimensions of 40 x 35 x 35 cm in width, length, and depth respectively. There are two parallel, circular, water-cooled metal plates, the plane surfaces of which are 17.7 cm in diameter, encircled with plastic covers that provide structural support. When the electric field applied to the plates reaches approximately 8.5 kV/cm at the proper frequency, an OAUGDP™ is initiated. At atmospheric pressure, the electric field is 2-3 kV/cm for argon and helium, and 8.5 kV/cm for air, well below the DC sparking electric field for the gas used. At least one or both electrodes have to be insulated to permit the charge build-up that maintains the plasma from one half-cycle of the RF to the next. The insulation material could be quartz, Pyrex, alumina, or glass, between 1 and 3 mm thick.

The OAUGDP™ can be operated over a wide range of experimental conditions. The RF high voltage power supply sub-system works from 1–20 kHz, and provides RMS voltages up to 20 kV. No vacuum system is necessary. The plasma is uniform and stable in a relatively large gap

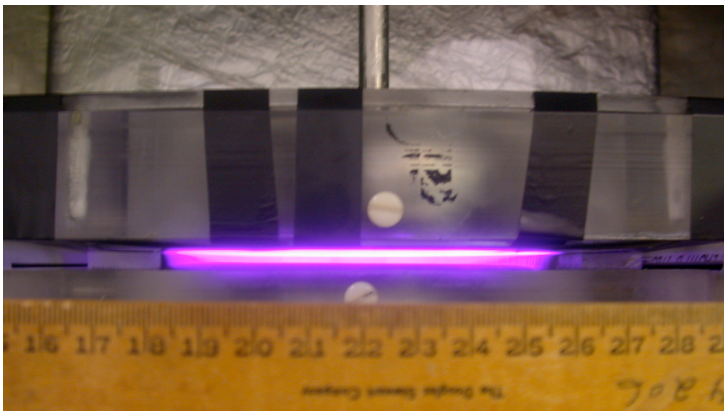

Figure 15 MOD VI OAUGDP™ Parallel Plate Re-circulating Plasma Reactor

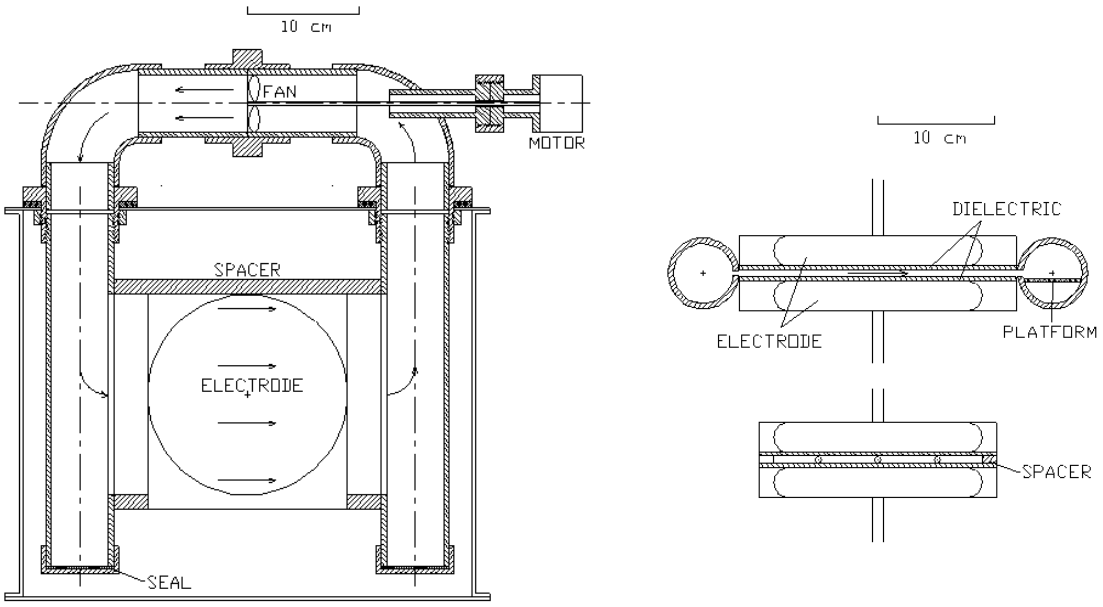

Figure 16 The Plan View and Elevation View of Mod VI OAUGDP Reactor

(2-5 cm) between the electrodes. For a given electrode gap separation, the RF frequency and RMS voltage were adjusted to produce a uniform glow discharge plasma without filamentation. As shown in Figure 15, the OAUGDP reactor is uniform without filamentary microdischarges, if the proper combination of gap distance, RF driving frequency, and RMS voltage is used. Operating parameters for the RF voltage in most experiments with the Mod VI Reactor were from 8.5 to 11 kV RMS, and from 5.0 to 7.0 kHz.

The plasma active species are designed to re-circulate in the Mod VI reactor, as shown in Figure 16. The plan view shows how the 15 cm diameter electrodes are fed by a re-circulating airflow from a slit in the plenum on the left. The airflow exits through a slit on the right, as indicated in the front and side elevations in Figure 16. The re-circulating airflow is driven by a fan in the upper section of the 5 cm diameter PVC pipe that forms the flow path.

For direct, re-circulating exposure, a planar sample is taped on the lower electrode of the Mod VI reactor. When the plasma is on, the sample is in direct contact with the plasma. It is bombarded by active species in the plasma and by active species carried in the re-circulating airflow. In the remote exposure mode, the sample is placed on a platform set up in the outlet plenum pipe, to the right of the plasma. Such a configuration assures

that in certain experiments when low-level exposure to the plasma is expected, only re-circulating active species are acting on the sample so as to reduce the power input to the material surface.

CHAPTER VII. PREVIOUS RESULTS FROM OAUGDP EXPOSURE OF POLYMERIC MATERIALS

At the UT Plasma Sciences Laboratory, it was found that etching of surfaces occurred [Tsai et al. 1997] in early experiments on the wettability and wickability of meltblown polymeric microfiber fabrics exposed to helium and argon OAUGDP plasmas. The mechanism of action appeared to be that adsorbed monolayers from the surface were removed by plasma bombardment and that removal was followed by erosion of the underlying polymeric material. Figure 17 is a SEM of polypropylene fibers before and after five minutes of direct exposure to a CO_2 OAUGDP [Tsai et al. 1997]. In this case, the duration of exposure has been sufficiently long that not only have the adsorbed monolayers of contaminants been removed, but also the roughened, post-exposure surface has been etched to a depth of about 100 nanometers.

In the untreated and treated PP meltblown fibers illustrated in the SEM photomicrographs of Figure 17, a significant change was observed on the surface roughness after plasma treatment [Tsai et al. 1997]. Three factors are believed to be responsible for the formation of surface roughness and microholes: 1.) the etching by plasma active species of the polymeric surface; 2.) chemical reactions with the active species; and 3.) the non-

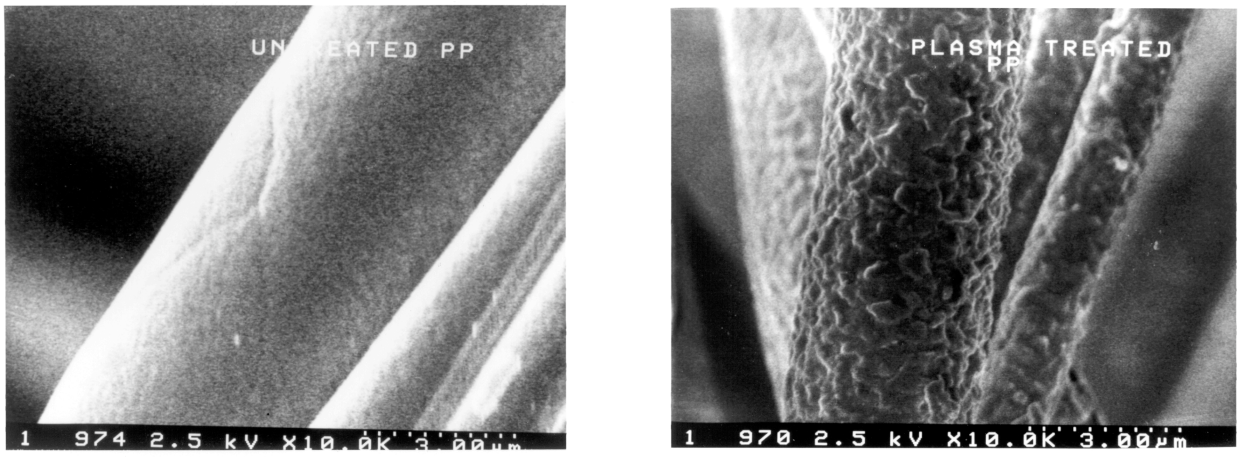

(a) **(b)**

Figure 17. SEM of Polypropylene (PP) Fibers: (a) untreated (b) fibers exposed for several minutes to an OAUGDP CO_2 plasma. Note three-micron fiduciary scale at the lower right.

uniform cooling rate after the surface is heated up by the plasma energy flux. The surface roughness results in enhancement of the filtration efficiency of a filter medium due to the increase of the fiber surface area. The etching also increases the dust-holding capacity by holding the dust in the roughened surface topography, which increases the filter service life.

Plasma exposure can also increase the surface energy, but "aging" or the durability effect was also observed for many materials tested [Tsai et al. 1994]. In most cases investigated, plasma-treated surfaces exhibit a wettability that decreases with time, usually effective up to a week after exposure. The duration might be sufficient for many industrial applications such as printing, dyeing, or adhesive bonding, where these operations are performed in-line within a few seconds of plasma exposure. For consumer products like clothing and diapers, however, durable wettability and wickability of at least six months are required.

CHAPTER VIII. EFFECTS OF PLASMA EXPOSURE ON THE TENSILE STRENGTH OF PU AND NYLON MICROFIBER FABRICS AND NANOFIBER FABRICS

To examine their macroscopic characteristics, both microfiber and nanofiber fabrics were subject to tests of tensile strength, surface energy, and aging effects after plasma exposure. In addition to data from fabrics with a different fiber size scale, we present data for both PU and Nylon, and we also present data from controls that were unexposed to the OAUGDP , and samples that were exposed for times ranging up to 120 seconds. No literature was found with respect to the normalized tensile strength of nanofiber fabrics.

First, selected groups of fabrics were tested in a Model SSTM-1-E-PC Unified Tensile Testing Machine (Figure 18) manufactured by the United Calibration Corporation (http://www.tensiletest.com), using the procedure for fabric samples described in ASTM Standard 5035-95. The purpose of this test is to measure the maximum force that the non-woven can support before rupture, thereby indicating how strong it is. In characterizing the micro- and nanofiber fabrics, all the specimens were prepared as rectangular strips 2.5 cm in width and 10 cm long, and the basis weight is obtained by dividing the sample weight by its area. We normalized the peak (failure) force to its basis weight in each test.

Figure 18 United Calibration Tensile Testing Machine Model SSTM

All the tabular data below represent the average of five samples taken under the same plasma operating conditions. In all of the tensile strength, surface tension, and wettability tests, the plasma operating conditions were held constant at 11 kV and 8kHz unless otherwise noted, and the samples were directly exposed to the plasma. We first report the data on the tensile strength of these materials, then the results of their surface energy and wettability tests after OAUGDP exposure.

As a point of reference, Table 3 shows the tensile strength of meltblown (MB) PU microfiber fabric samples 2.5 x 10 cm^2 in dimensions. Within the standard deviation, exposure to the plasma had no significant detrimental effects on the strength of this material.

These tests were followed by similar tests on the standard sized samples of electrospun nanofiber fabric, the results of which are listed on Table 4. No durations longer than ten seconds are listed because of currently unresolved problems with the exposure technique. The data on both Tables 3 and 4 are plotted on Figure 19, along with the error bars based on the standard deviation of the data. It shows a statistically significant result (beyond the error bars), that the electrospun PU fabric is at least twice as strong per unit areal weight as the meltblown material. However, a significant (beyond the error bars) decrease in strength occurred for the electrospun PU fabric. This result is expected because of the etching or erosion of the fibers due to plasma exposure, according to previous results discussed in Chapter VII.

Table 3 Tensile Strength of MB PU Microfiber Fabrics (2.5x10 cm^2)

Treatment time (s)	Basis Weight. (g/sqr. m)	Break Elong (%)	Peak Force (N)	Normalized P.F.	S.D.	C.V.(%)
control	27.9	357	5.43	0.194	0.018	9.4
3	28.2	306	4.78	0.169	0.026	15.4
10	31.7	247	4.90	0.154	0.034	22.2
30	28.1	316	4.37	0.155	0.020	12.6
60	28.6	288	4.81	0.171	0.031	18.4

Table 4 Tensile Strength of PU Nanofiber Fabrics (2.5x10 cm^2)

Treatment time (s)	Basis Weight (g/sqr. m)	Break Elong (%)	Peak Force (N)	Normalized P.F.	S.D.	CV(%)
control	38.2	163	18.6	0.479	0.066	13.8
5s	41.9	188	19.2	0.432	0.109	25.3
10s	28.2	214	8.4	0.286	0.069	24.3

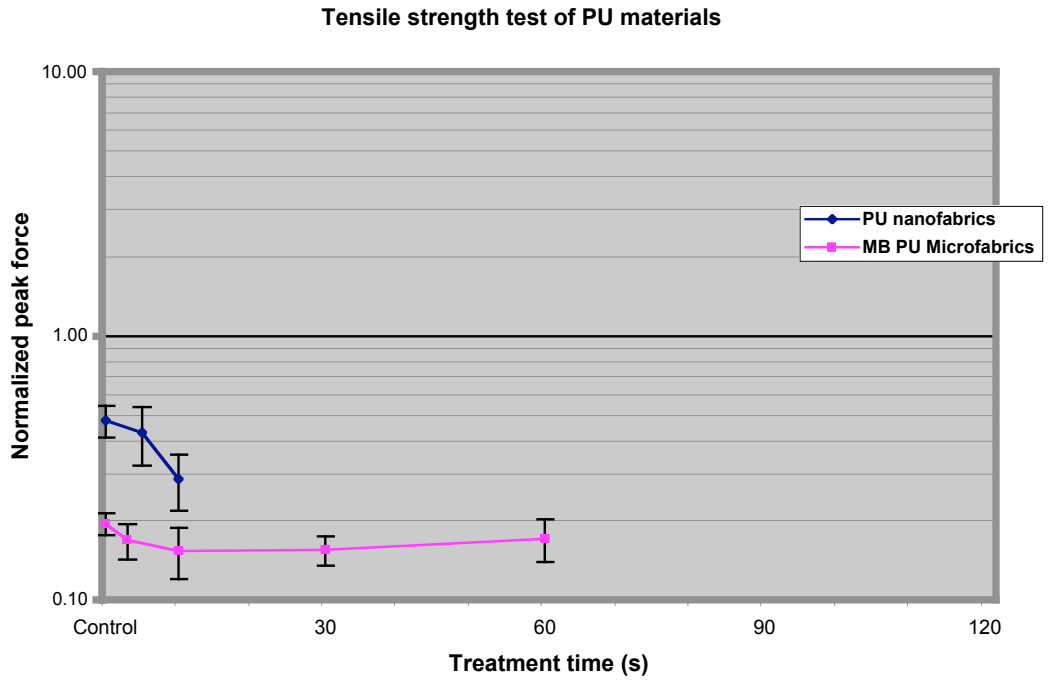

Figure 19 Normalized Peak Force as a Function of OAUGDP Treatment Time for PU Microfiber and Nanofiber Fabrics

To move on to Nylon, Table 5 shows the tensile strength of meltblown (MB) Nylon microfiber fabric samples 2.5 x 10 cm^2 in dimensions. Within the standard deviation, exposure to the plasma had no significant detrimental effects on the strength of this material. There may be a trend to slightly greater strength with plasma exposure, although the effect quickly saturates if it is present at all.

These tests on Nylon microfiber fabric samples were followed by similar tests on 2.5 x 10 cm^2 samples of electrospun Nylon nanofiber fabric, the results of which are listed in Table 6. Again, no durations longer than ten seconds are listed because of currently unresolved problems with the exposure technique. The tensile strength of the unexposed nanofiber material is about ten times that of the unexposed Nylon microfiber fabric, a result far outside the standard deviation of the data. Plasma exposure might have slightly changed the normalized peak force at the point of material failure. Again, this could have resulted because the small fiber diameter of ES Nylon fabric was etched proportionally more than that of either PU fabrics.

The data on both tables are plotted on Figure 20, along with the error bars based on the standard deviation of the data. These data support the trends discussed in connection with the two tables, particularly the ten-fold higher normalized peak failure force for the Nylon nanofiber fabrics, and the absence of significant loss of the initial strength after plasma exposure.

Recall the discussion of SEM images in previous chapters and we may conclude that the higher strength of ES fabrics results from the random weaving, knotting, and nodal attachment of the ES fibers.

Table 5 Tensile Strength of MB Nylon Microfiber Fabrics (2.5x10 cm^2)

Treatment time (s)	Basis Weight (g/sqr. m)	Break Elong (%)	Peak Force (N)	Normalized P.F.	S.D.	CV(%)
Control	40.4	24.9	6.24	0.154	0.021	13.6
3	44.2	20.8	7.92	0.179	0.029	15.9
10	44.7	22.2	8.50	0.190	0.015	7.8
30	44.7	20.2	7.83	0.175	0.026	15.0
60	44.0	19.5	7.77	0.176	0.007	3.8
120	40.7	25.6	6.58	0.162	0.015	9.4

Table 6 Tensile Strength of Nylon Nanofiber Fabrics (2.5x10 cm^2)

Treatment time (s)	Basis Weight (g/sqr. m)	Break Elong (%)	Peak Force (N)	Normalized P.F.	S.D.	CV(%)
control	7.6	6.8	11.7	1.52	0.09	6.0
5	15.4	10.7	26.3	1.68	0.30	17.6
10	12.0	8.2	15.1	1.23	0.34	27.3

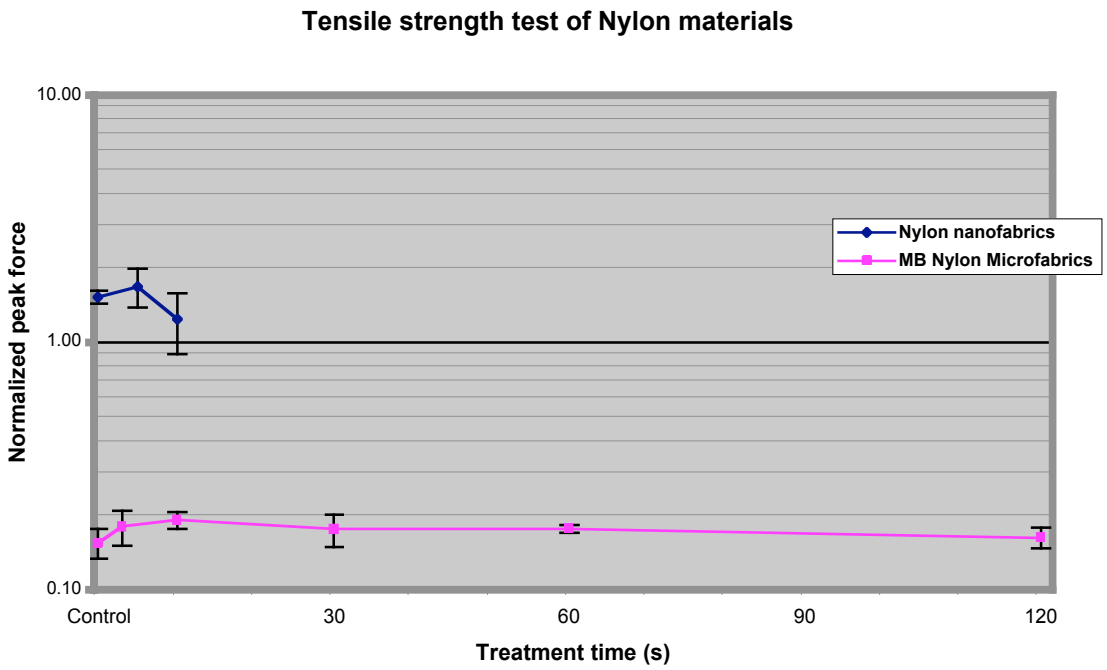

Figure 20 Normalized Peak Force as a Function of OAUGDP Treatment Time for Nylon Microfiber and Nanofiber Fabrics

CHAPTER IX. METHODS FOR SURFACE ENERGY MEASUREMENT

Wettability is one of the most important characteristics of fibrous materials such as paper or fabrics. It is the ability to adsorb a liquid on a solid surface, or to absorb it into the bulk, and it can be measured in terms of surface energy.

In nature, the surface energy is the work done against surface tension forces in creating a unit area of liquid on the surface at constant temperature. Consider a liquid droplet on the surface. The liquid surface will tend to contract to form a sphere because those molecules on the surface are attracted inward by interior molecules through atomic forces. However, the surface tension of the solid surface is acting to pull the liquid away in all directions and therefore spread it. As a result, the equilibrium of these two forces determines the behavior of a liquid on a surface, visually the shape of a droplet.

The sessile liquid drop test is one of the methods based on the above principle to measure the surface energy/tension. First, a single drop of liquid, usually distilled or de-ionized water, is placed on a horizontal workpiece. Then the contact angle is measured, which is the angle included between the tangent plane to the surface of the liquid and the tangent plane to the surface of the solid as shown in Figure 21. Sometimes an advancing or receding contact angle is measured, depending upon the nature of the surface material.

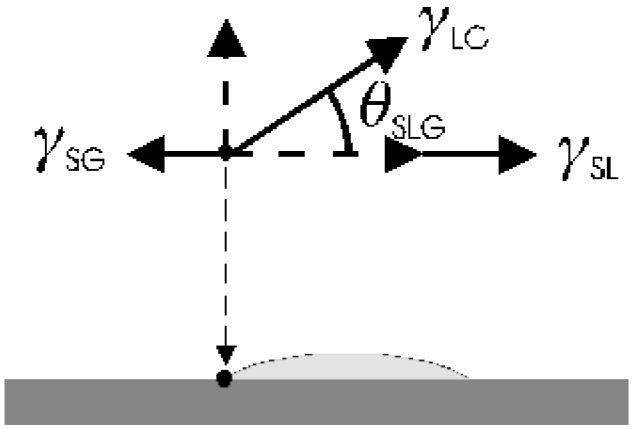

Figure 21 Contact Angle of a Liquid Drop on a Surface

The sessile liquid drop test provides a quantitative measure of wettability. If the surface is unwettable, the liquid drop forms hemispherical beads with a high contact angle and have a minimum contact area with the surface; if wettable, the drop flattens and spreads over a relatively large area with a low contact angle. Generally, an angle of 50 degrees or higher indicates that the surface is unwettable, while 10 degrees or below is very wettable.

In actual measurements, a contact angle meter manufactured by TANTEC USA Inc. is used. The experimental setup and procedures are shown in Figure 22 (http://www.tantecusa.com). A piece of fabric sample is placed on a platform, which is in the light path of an optical system. The eye dropper, from which the liquid is released, is aimed at the workpiece

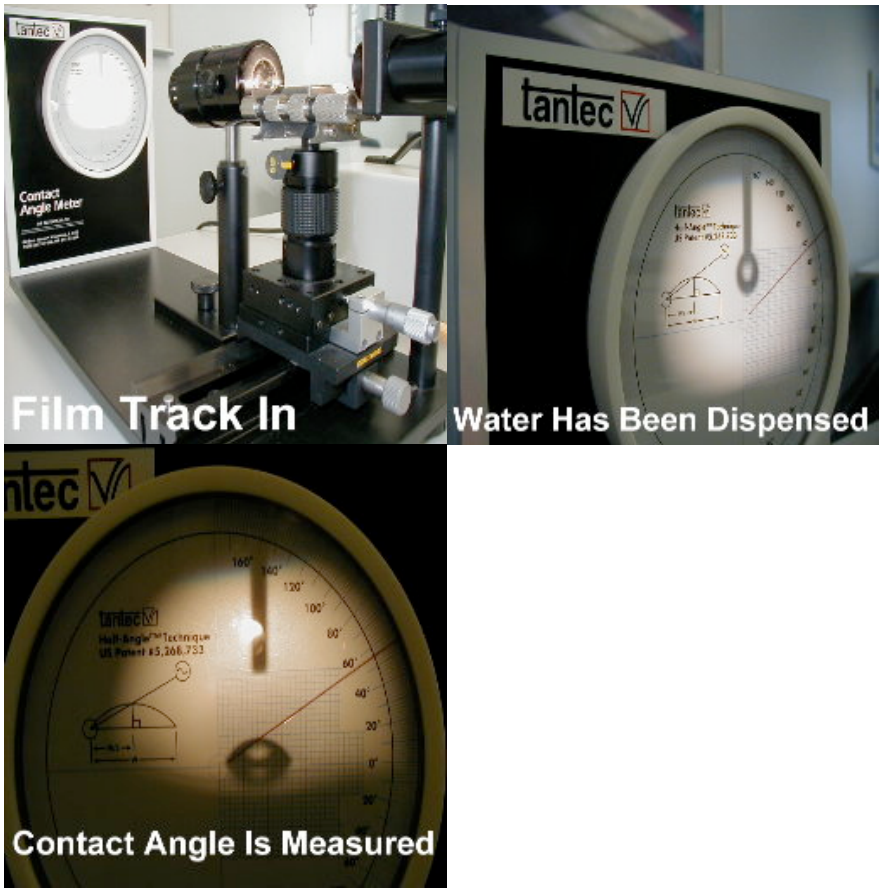

Figure 22 Contact Angle Measurement on a Contact Angle Meter

from immediately above. Once the droplet is formed and has stabilized on the sample surface under test, an enlarged image of this liquid drop is projected on a screen containing a protractor. Now the contact angle can be read from the circumferential protractor. It is important to take more than one measurement for a single data point to obtain a statistically better result.

Another widely used method for surface energy measurement is called the dyne level test, according to ASTM Standard D25781. This method is the most convenient and effective to determine the surface energy of plastic films and other non-absorptive substrates. There is a set of commercially available liquids for which each container of liquid has a surface tension specified by its vendor. The measurement ranges from 30 to 70 dynes/cm with a resolution of 1 or 2 dynes/cm (dynes/cm, equivalent to 10^{-3}N/cm, is the unit of surface tension in the CGS system). A line or droplet of such liquid with a given surface energy/tension level is placed on the surface to be tested. If the droplet holds its shape for more than 3 seconds, the surface tension/energy of this surface is lower than that of the solution used. By continuing to test different solutions in a sequence until one wets the surface, the surface energy level under test will be ultimately determined. The location of test on the sample must be changed after each such measurement. For more information on this method, see http://www.accudynetest.com/qctest.html.

Figure 23 presents three solutions from a series of the ACCU DYNE surface tension test fluids produced by Diversified Enterprises Inc., and their respective effects on two fabric samples. The sample in the middle is a Nylon meltblown fabric that has been exposed to plasma for 5 seconds. Its surface energy is above 70 dyne/cm, as is shown. The surface energy of its control (lower strip), a Nylon MB fabric without plasma treatment, however, is between 50 and 60 dyne/cm.

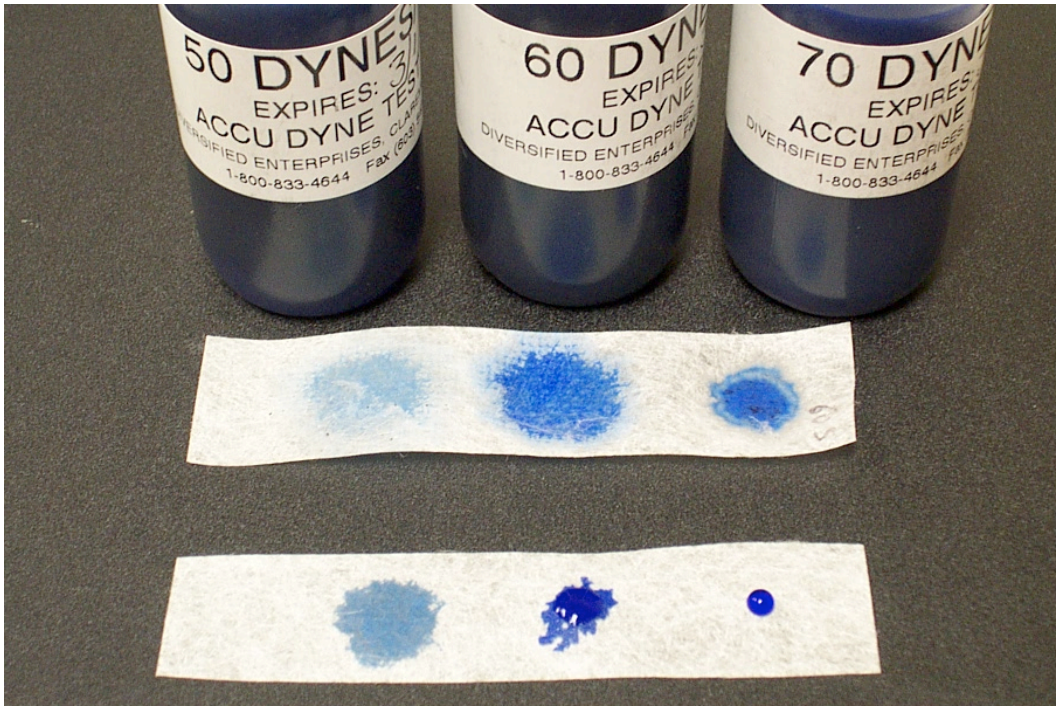

Figure 23 Dyne Test Liquids and Test Demonstration on Nylon Microfiber Fabric Samples: (upper) Plasma-treated and (lower) Control

CHAPTER X. EFFECTS ON THE SURFACE ENERGY CHARACTERISTICS OF PU AND NYLON MICRO- AND NANOFIBER FABRICS

Previous work has shown that it was particularly difficult to increase the surface energy of PP and PE and to render any increases durable in time [Tsai et al. 1994, Roth et al. 2000]. This is likely due to their chemically inert nature and their non-polar properties, in contrast to PET and Nylon. With recent improvements in the plasma reactor, such as recirculating air flow and impedance matching, the surface energy of meltblown PP fabric was increased from 35 dynes/cm to 72 dynes/cm by OAUGDP™ treatment for periods as short as one second. However, the surface energy decreased with time during the first few days and then leveled off at values greater than the untreated material, indicating a significant aging effect.

As a point of reference, Table 7 shows the contact angle of meltblown (MB) PU microfiber fabric samples. The rows of the table are sorted by plasma exposure time durations, and the columns for aging periods after exposure. As seen in the table, the controls were very unwettable, with a contact angle of about 121 degrees. Exposure to the OAUGDP™ reduced this value significantly to lower and commercially interesting values, about 60 degrees, but after only one day it returned to higher levels. The decreased contact angle, however, was relatively durable for all but the shortest exposure times and the longest times after exposure. The wettability and small contact angles observed before 24 hours elapsed may be of interest commercially.

Table 8 shows the surface energy in dynes/cm measured by the Dyne level test for meltblown Nylon microfiber fabric as a function of the time of exposure to the plasma (the rows of the Table) and the time after exposure (the columns of the Table). The surface energy increases from 48 dynes/cm to at least 70 dynes/cm, the highest value we can measure with this method, for plasma exposure time as short as 3 seconds. The result of the aging test is more encouraging: for all but the shortest exposure times, the high surface energy remains durable for at least 56 weeks after exposure. Even after a year, the surface energy of fabrics does not drop too much. The lowest observation occurs in the fabrics treated for 5 seconds, whose surface energy is 64 dynes/cm, still water wettable and well above that of its control. In industry, a shelf life exceeding around six months is preferable for commercial products, during which they should not exhibit any significant

Table 7 Liquid Drop and Aging Contact Angles of Meltblown PU Microfiber Fabrics: Before (Control) and After OAUGDP Treatment at 8 kHz and 6.0 kV rms

	Aging time after exposure					
Exposure Time, sec	**Control**	**5 minutes**	**24 hours**	**48 hours**	**72 hours**	**1 week**
5s	121°	Varying from 56° to 98°	69°	77°	75°	78°
10s	121°	49°, down to 10°	62°	75°	75°	79°
20s	121°	Absorbed, <10°	72°	73°	77°	78°
30s	121°	Absorbed immediately	60°	60°	64°	66°
60s	121°	Absorbed immediately	48°	46°	47°	58°

Table 8 OAUGDP Surface Energy in Dynes/cm of Meltblown Nylon Microfiber Fabrics: at 8 kHz and 5.5 kV (as of October 29th, 2003)

Aging Time / Exposure Time, sec	Control	5 minutes	24 hours	2 weeks	27 weeks	56 weeks
3s	48	>70	70	68	-	-
5s	48	>70	>70	70	70	64
10s	48	>70	>70	>70	>70	66
20s	48	>70	>70	>70	>70	68
30s	48	>70	>70	>70	>70	70
60s	48	>70	>70	>70	>70	>70

aging effect. This is the first time that such a durable high surface energy of polymeric fabrics by exposure to an air plasma is reported.

The results of surface energy tests are somewhat ambiguous due to the testing methods we have been using so far, the sessile liquid drop test or Dyne level test, on a difficult material like nanofiber fabrics. The contact angle or liquid droplet usually advances on the fabric surface or permeates the thin fabric layer, which could be seen as "absorbed," for untreated materials. One explanation might be that the residue of electrospinning solution chemicals is wettable. If the test samples are heated to a high temperature, depending on the material, for a period of time like tens of minutes, those chemicals should be removed; therefore the effect of such a residue on this measurement will be ruled out.

A sample of the surface energy data we have for PU, Nylon 6, and Nylon 6-6 nanofiber fabrics is illustrated in Table 9. The surface energy of both materials is relatively high before plasma exposure, as is seen in the column of "as received". Because of the reasons we specified earlier like residues, the fabrics are then water-washed and heated at 100 °C for 60 minutes to remove those influences. The control values after these treatments drop to the range close to those of MB fabrics in the same material. Therefore, the difference of surface energy of control and plasma-

Table 9 Surface Energy of Nanofiber Fabrics: Before and After OAUGDP Treatment (Unit: Dyne/Cm)

Fabric Type	As received	Control	5 seconds	10 seconds
Nylon 6	62	52	>70	>70
Nylon 6-6	62	54	>70	>70
PU	70	50	>70	>70

treated fabrics should be accounted for. Also, as can be seen, the surface energy of all the samples reaches the highest value we can measure after only five seconds of treatment. It appears that all the nanofiber fabrics we have tested can be made quite wettable with a very brief direct exposure to the OAUGDP .

With the surface energy of fabrics increased, its moisture vapor diffusion resistance is reduced. Body heat can be dissipated through the ventilation of the sweat vapor more efficiently. Therefore, the increase of fabric wettability for protective clothing improves the body comfort.

CHAPTER XI. CONCLUSIONS AND PROSPECTUS

SEM images and fiber diameter data are taken from both microfiber and nanofiber fabrics made of various materials. It is strongly suggested that the electrospinning process has caused major structural changes in these nanofiber fabrics, compared to the microfiber fabrics made by meltblowing technology, and therefore affected many bulk characteristics of the nanofiber fabric material.

Our data show that the strength of unexposed (to plasma) PU nanofiber fabric is about two times that of microfiber fabric, and that the strength of unexposed Nylon nanofiber fabric is about ten times that of Nylon microfiber fabric. When exposed to the OAUGDP , the meltblown microfiber fabrics do not degrade significantly in normalized strength with plasma exposure times up to 120 seconds. There is a small but insignificant degradation in strength of plasma-exposed electrospun nanofiber fabrics, however.

Our data also indicate that the surface energy or wettability of both PU and Nylon micro- and nanofiber fabrics are greatly increased by exposure to an air OAUGDP . The high surface energy thus imparted to the Nylon meltblown fabrics is durable for over a year.

In conclusion, electrospun nanofiber fabrics have several potentially attractive features. Among these are a very soft hand; the potential of acting as a barrier against microorganisms and fine particulates; a potentially good strength per unit weight; a high surface energy that indicates a potentially good moisture vapor transmission rate; the potential of being fabricated at room temperature with robust, simple capital equipment; and a potentially low energy requirement for production.

Future work is expected to be done in increasing the fabric production rate, performing more sample tests that give better statistical results, better understanding of the process of fiber formation, therefore the improvement of fabric uniformity, and different solution materials that may find other promising results.

LIST OF REFERENCES

LIST OF REFERENCES

Ben Gadri, R., 1999, "One Atmosphere Glow Discharge Structure Revealed by Computer Modeling," *IEEE Trans. Plasma Sci.*, Vol. 27, No. 1, pp 36-37.

Chen, W., Li, X., Tsai, P. P.-Y., and Roth, J. R., 2003a, *"Effect of Exposure to a One Atmosphere Uniform Glow Discharge Plasma(OAUGDP) on the Surface Energy and Strength of Nanofiber Fabrics"*, Paper 3PA53, Proceedings of the 30th IEEE International Conference on Plasma Science, Jeju, Korea, June 2-5, 2003, Page 298, IEEE Catalog Number 03CH37470, ISBN 0-7803-7011-X.

Chen, W., Li, X., Tsai, P. P.-Y., and Roth, J. R., 2003b, "Investigation of Meltblown Microfiber and Electrospun Nanofiber Fabrics Treated with A One Atmosphere Uniform Glow Discharge Plasma (OAUGDP™)", Paper NWP .056, Presented at the 56th Annual Gaseous Electronics Conference 2003, October 21-24, San Francisco, CA.

Davis, M., 1987, "Electrostatic Melt Spinning Process Delivers Unique Properties," Nonwovens World, Vol. 9, 51 (1987).

Formhals, A., 1934, "Process and Apparatus for Preparing Artificial Threads," US Patent 1,975,504.

Gibson, P., Rivin, D., Kendrick, C., Schreuder-Gibson, H., 1999a, "Humidity-Dependent Air Permeability of Textile Materials", Text. Res. J., 69(5), 311(1999).

Gibson, P. W., Schreuder-Gibson, H.L., Rivin, D., 1999b, "Electrospun Fiber Mats: Transport Properties," AIChE J., 45(1), 190 (1999).

Haynes, B. D., 1991, "An Experimental and Analytical Investigation on The Production of Microfibers Using a Single Hole Melt Blowing Process", Ph.D. Dissertation, the University of Tennessee.

Ko, F. K., Kawabata, S., Inoue, M., Niwa, M., Fossey, S. and Song, J., 2002, "Engineering Properties of Spider Silk", Proceedings, MRS 2001 Fall Meeting, Hynes Convention Center and Sheraton Boston Hotel, Boston, Massachusetts, November 26-30, 2001, MRS, 2002.

Noll, Amanda, 2000, Fabric Project in Scanning Electron Microscopy 2076-572, of Professor Bruce E. Kahn, bekpph@rit.edu, http://www.rit.edu/~bekpph.

Roth, J. R., Tsai, P. P.-Y., Liu, C., Laroussi, M., and Spence, P. D., 1995a, *One Atmosphere Uniform Glow Discharge Plasma,* U. S. Patent No. 5,414,324, Issued May 9, 1995.

Roth, J. R., 1995b, *Industrial Plasma Engineering: Volume 1, Principles*, Institute of Physics Publishing, Bristol and Philadelphia, ISBN 0-7503-0318-2.

Roth, J. R., Tsai, P. P.-Y., Liu, C., Wadsworth, L. C., 1995c, *One Atmosphere Uniform Glow Discharge Plasma,* U. S. Patent No. 5,456,972, Issued Oct 10, 1995.

Roth, J. R., Chen, Z., Sherman, D. M., Karakaya, F., Tsai, P. P.-Y., Kelly-Wintenberg, K., and Montie, T. C., 2000, "Increasing the Surface Energy and Sterilization of Non-woven Fabrics by Exposure to a One Atmosphere Uniform Glow Discharge Plasma (OAUDGP)" , Proc. Int. Nonwovens Techinical Conf. INTC-2000 (Dallas ,TX)

Roth, J. R., 2001, *Industrial Plasma Engineering: Volume 2, Applications to Nonthermal Plasma Processing,* Institute of Physics Publishing, Bristol and Philadelphia, ISBN 0-7503-545-2.

Roth, J. R., Chen, W., and Tsai, P. P.-Y., 2003, "Investigation of Meltblown Microfiber and Electrospun Nanofiber Fabrics Treated with A One Atmosphere Uniform Glow Discharge Plasma (OAUGDP™)", Presented at the 13th Annual International TANDEC Nonwovens Conference November 18-20, 2003, Knoxville, TN.

Schmidt, K., 1980, "Manufacture and Use of Felt Pads Made from Extremely Fine Fibres for Filtering Purpose," Melliand Textilber., 61, 495 (1980).

Schreuder-Gibson, H., Gibson, P., Senecal, K. and Tsai, P., 2000, "Protective Materials Based on Electrospun Nanofibers," 39th International Man-made Congress, Dombirn/Austria, Sept. 13 – 15, 2000.

Tsai, P. P.-Y., Wadsworth, L. C., Spencer, P. D., and Roth, J. R., 1994, "Surface Modification of Non-woven Webs Using a One-Atmosphere Glow Discharge Plasma to Improve Web Wettability and Other Textile Properties", Proc. 4th Ann. TANDEC Conf., Knoxville, TN.

Tsai, P. P.-Y., Wadsworth, L. C., and Roth, J. R., 1997, "Surface Modification of Fabrics Using a One-Atmosphere Glow Discharge Plasma to Improve Fabric Wettability", *Textile Research Journal*, Vol. 67, No. 5, pp. 359-369.

Tsai, P. and Schreuder-Gibson, H., 2001a, "Methods and Apparatus for Electrostatic Fiber Spinning'" patent filed to The University of Tennessee Research Corporation, April, 2001.

Tsai, P., and Schreuder-Gibson, H., 2001b, "Effect of Electrospinning Material and Conditions Upon Residual Electrostatic Charge of Polymer Nanofibers," 11th TANDEC Conference, The University of Tennessee, Nov. 4 –7, 2001.

Tsai, P., Schreuder-Gibson, H., and Gibson, P., 2002a, "Different Electrostatic Methods for Making Electret Filters," Journal of Electrostatics, 54(2002).

Tsai, P. P.-Y., Chen, Z., Chen, W., Li, X., and Roth, J. R., 2002b, *"Improving the Properties of Protective Clothing by Exposing Nanofiber Webs to a One Atmospheric Uniform Glow Discharge Plasma (OAUGDP)"* Presented at the Fall-2002 Fiber Society Conference, Natick Crowne Plaza Hotel, Natick, Massachusetts, October 16-18,2002.

Tsai, P. P.-Y., Chen, W., Li, X., and Roth, J.R., 2002c, "*Improving the Properties of Protective Clothing by Exposing Nanofiber Webs to a One Atmospheric Uniform Glow Discharge Plasma (OAUGDP)*", Presented at the 12th International TANDEC Nonwovens Conference, Knoxville, Tennessee, November 19-21, 2002.

von Engle, A., Seeliger, R., and Steenback, M., 1933, On the Glow Discharge at High Pressure, *Zeit. für Physik*, Vol. 85, 144 (1933).

Weghmann, A., 1982, "Production of Electrostatic Spun Synthetic Microbre Nonwovens and Applications in Filtration," Proceedings of the 3rd World Filtration Congress, Filtration Society, London (1982).

Zhang, D., Sun, C., Beard, J., and Zhao, W., 2001, "Characterization of Poly(Trimethylene Terephthalate) Meltblown and Spunbonded Nonwovens", Proceedings of 11th TANDEC Nonwovens Conference, The University of Tennessee, Knoxville, TN, USA, November 6-8, 2001.

VITA

Weiwei Chen was born on October 31st, 1979 in Huangshan, Anhui, People's Republic of China. He moved to Shanghai later and received a B.S. in Electrical Engineering from Northeastern University (Shenyang, Liaoning) in July 2001. In August 2001, he began pursuit of a Master of Science degree in the Department of Electrical & Computer Engineering at the University of Tennessee, Knoxville. He has served as a Graduate Teaching Assistant from 2001 to 2002 and a Graduate Research Assistant thereafter. He is currently an IEEE student member.